Supplementary material for

Orders of magnitude higher photoelectricity-ROS conversion efficiency of ubiquitous nanoscale natural ferralsol iron oxides than the synthetic ones: implication for their unexpected strong blocking-up of dissemination of antibiotic resistance in aquatic environment

Yutong Meng[1], Xiangliang Pan[1,2]*

[1] Key Laboratory of Microbial Technology for Industrial Pollution Control of Zhejiang Province, College of Environment, Zhejiang University of Technology, Hangzhou, China

[2] Xinjiang Key Laboratory of Environmental Pollution and Bioremediation, Xinjiang Institute of Ecology and Geography, Chinese Academy of Sciences, Urumqi, China

This supplementary material contains 4 texts, 6 tables, and 3 figures.

Text S1 Preparation of α-Fe_2O_3 nanoparticles and α-FeOOH nanorods

The α-Fe_2O_3 nanoparticles were purchased from Aladdin Co., Ltd (Shanghai, China) and used without further purification.

The α-FeOOH powders were synthesized via a facile hydrothermal method.[1] All the raw materials used were analytically pure chemical reagents without further treatment. First, the solution of 1 mmol ferric sulfate was titrated by the solution of 9 mmol NaOH. Second, the obtained precipitates and aqueous solution were moved into a 25 ml Teflon liner with the addition of 0.2 g Cetyl trimethyl ammonium Bromide (CTAB) as surfactant. Then, the mixture was hydrothermally reacted at the temperature of 180 ºC for 2 h to synthesize single-phase α-FeOOH powders, and the specimens obtained were washed by deionized water and absolute ethyl alcohol for several times. After the specimens were cleaned and dried, grind them in an agate mortar to obtain the fine powder.

Text S2 Soil particles classification

According to the soil particle classification method,[2] the sediment particles were classified as follows.

(i) Gravel (>250 μm). Sediment of 50.0 g was passed through a 60-mesh sieve. The residue on the sieve was gravel (>250 μm), and the sieved fraction (< 250 μm) was used for further classification.

(ii) Fine sand (50–250 μm). The sieved fraction was loaded into a beaker with 1.0 L of deionized water and dispersed for 10 min under ultrasonic treatment. Then, the suspension was passed through a 300-mesh sieve and washed with 400 mL of deionized water. The residue on the sieve was fine sand. The sieved fraction (< 50 μm) was collected for further classification.

(iii) Silt (5–50 μm). The suspension obtained in the step[3] was transferred into a 2.0-L beaker with 1.6 L of deionized water (approximately 13 cm in depth). The suspension was completely mixed with a glass stirring rod for 5.0 min and then began to settle without any disturbance. According to the Stokes' law, settling time of 74 min was required for particles of > 5 μm. After 74 min, 1.3 L of overlying water was drained by siphon. Then, 1.3 L of deionized water was replenished for another 74 min of settlement. The above steps were repeated 3–5 times until the supernatant was free of turbidity. The settled solids in the beaker bottom were silt (5–50 μm). All the drained overlying water (containg particles of < 5 μm) was combined for further classification.

(iv) Fine silt (1–5 μm). Five milliliters of the above overlying water was centrifuged (TGL-15B, Shanghai Anting, China) at 2000 rpm (relative centrifugal force, RCF = 430 *g*) for 7.0 min. After centrifugation, the pellet was fine silt with a diameter of 1 to 5 μm, and the supernatant containing particles of < 1 μm was collected and freeze-dried for further treatment (see Text S3).

The centrifugation time was calculated by the following formula:

$$Ts = \frac{27.4 \times \ln \frac{R_{\max}}{R_{\min}} \mu}{n^2 r^2 (\sigma - \rho)} (\min) \quad (1),$$

where *Ts* is the centrifugation time; "$\sigma - \rho$" represents the density difference between sediment particles and water (g/cm^3), and 1.65 g/cm^3 is adopted; μ represents the water viscosity coefficient (0.01005 g/cm/s at 20 °C); *n* represents revolution speed (rpm); *r* represents the radius of particle (cm); and R_{max} and R_{min} represent the horizontal distance from the axis of the centrifuger to the liquid bottom and surface, respectively (cm).

Text S3 Natural iron mineral purification

Add the submicron-colloidal soil particles (< 1 μm) of 0.1-0.5 g into several 50-ml Teflon crucibles, add hydrogen peroxide to remove organic matter, heat to remove excess hydrogen peroxide. 40 ml of 5 M NaOH was added in each crucibles,[4-6] the mixture was boiled at the temperature of 120 ºC for two hours to remove silicate, silicoaluminate, silica, etc. After filtering to obtain solid nanoparticles, wash the sample twice with 0.5 M HCl (20 min of contact) to remove sodalite, once with 0.1 M hydroxylamine hydrochloride to clean manganese oxide and heavy metals,[7] and twice with deionized water. Subsequently, use a strong magnet (1.4 T) to absorb weakly magnetic iron oxides[8] and freeze-dry them for experiments.

Instructions for filtration: use suction filtration device, 0.1 μM PTFE filter membrane, intercepting nanoparticles. After the filtration, place the filter membrane into a centrifuge tube and add the solvent required in the above steps. Ultrasound for 10 minutes (with appropriate

scraping) to separate the nanoparticles from the filter membrane and thoroughly mix with the solvent, ensure that there are no large particles. When carrying out the next cleaning step, change the required solvent and perform a similar suction filtration step.

Instructions for magnetic attraction: utilize the weak magnetism of iron oxides to further purify nanoparticles through magnetic attraction. Use a long, strong magnetic magnet, make a slight height difference between the two ends of the magnet, Start pouring the nanoparticle solution from a high position and make the solution flow across the cross-section of the magnet. Repeat several times, and collect the particles adsorbed on the magnetic cross-section.

Text S4 Iron oxide characterization

Powder X-ray diffraction (PXRD) analysis was performed by a Rigaku Smartlab-9KW diffractometer with Cu-Kα radiation (λ = 0.15406 nm) at a current of 40 mA and a voltage of 40 kV. X-ray photoelectron spectroscopy (XPS) and valence band-X-ray photoelectron spectroscopy (VB-XPS) were obtained on a Thermo Scientific K-Alpha instrument with a monochromatic Al Kα source. The electrochemical measurements were performed following the procedure described in a previous publication[9] but change "1 mg MOFs was dispersed in 2 mL ethanol containing 33 μL Nafion" to "3 mg of nanoparticle was dispersed in 550 μL of ethanol containing 50 μL Nafion". Photocurrent measurements were conducted in a three-

electrode system (0 V vs. Ag/AgCl reference, Pt counter electrode) with 0.1 M Na_2SO_4 electrolyte under AM 1.5G illumination (1000 W/m^2).

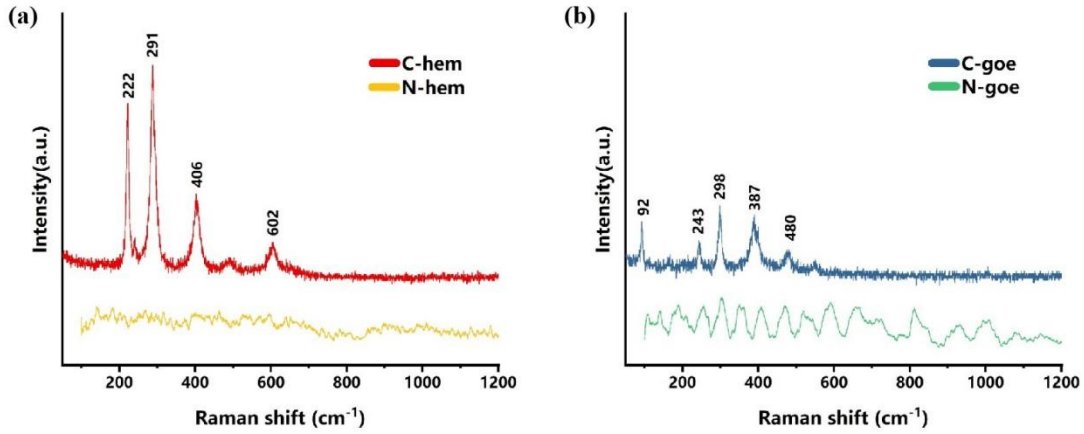

Fig. S1. Raman spectra of (a) N-hem and C-hem, (b) N-goe and C-goe. Due to long-term weathering and aging, NNIOs did not exhibit good peak while the synthetic materials exhibit good peak.

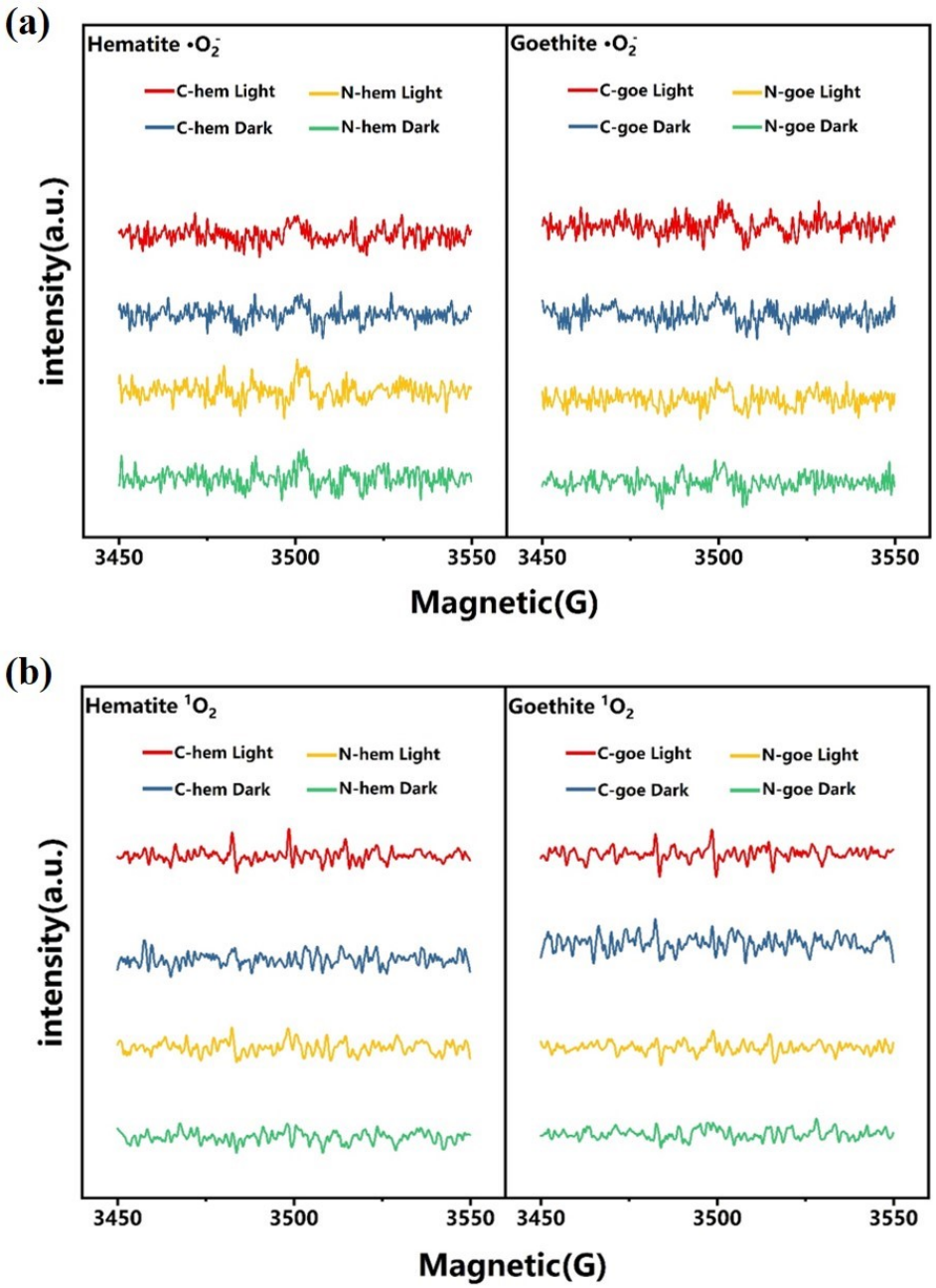

Fig. S2. EPR spectra of (a) DMPO/ O_2•- adduct, (b) TEMP/$^1O_2$ adduct in four kinds of iron oxide solutions measured right after illumination or after illumination, leave in dark for another 30 minutes.

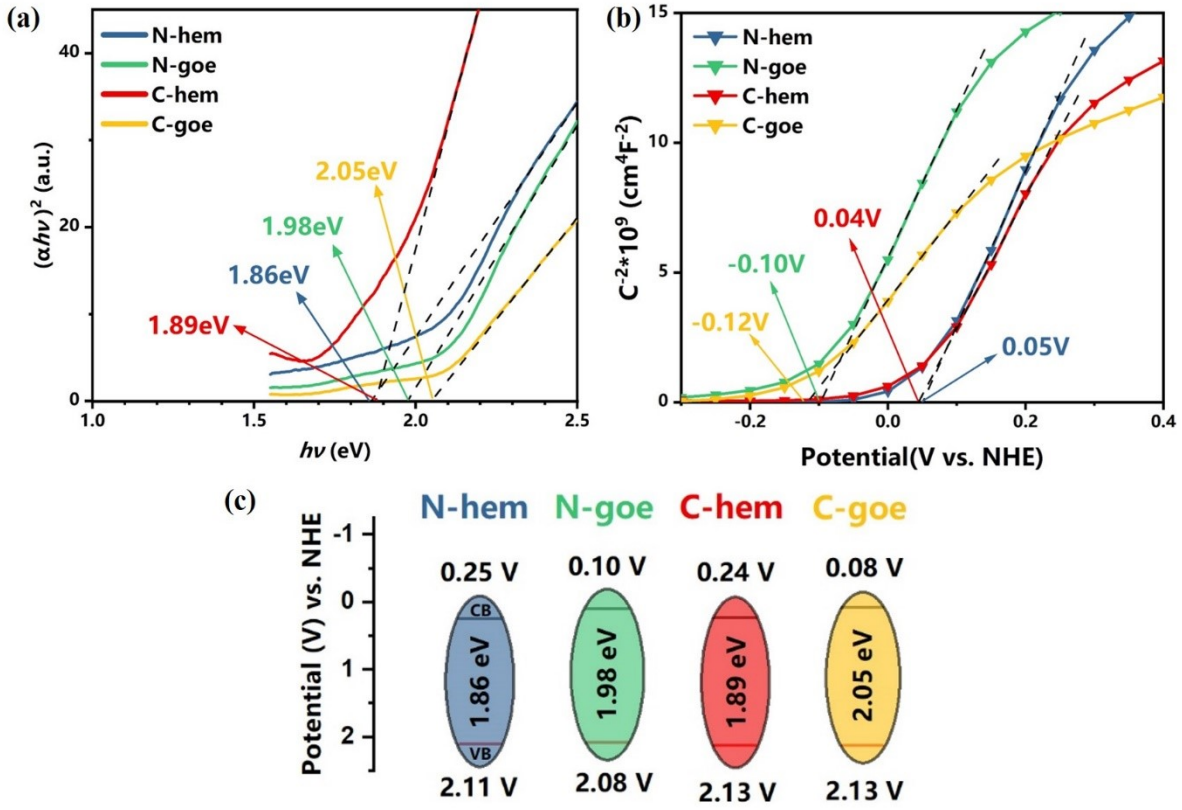

Fig. S3. (a) Tauc plots, (b) Mott–Schottky plots, (c) Band-structure characterization of N-hem, N-goe, C-hem, C-goe.

Table S1 C_t values and log_{10}(copies) data of 10-fold dilution method

Sample Name	Target Name	C_t	Copies	log_{10}(copies)
M-0	AMPR	8.556077	2352373290.43	9.37150624
M-0	AMPR	8.31573296	2352373290.43	9.37150624
M-1	AMPR	11.1768646	235237329.04	8.37150624
M-1	AMPR	11.0923681	235237329.04	8.37150624
M-2	AMPR	14.4460735	23523732.90	7.37150624
M-2	AMPR	14.7593117	23523732.90	7.37150624
M-3	AMPR	18.1401443	2352373.29	6.37150624
M-3	AMPR	18.2365665	2352373.29	6.37150624
M-4	AMPR	21.8466816	235237.33	5.37150624
M-4	AMPR	21.7944031	235237.33	5.37150624
M-5	AMPR	24.9625874	23523.73	4.37150624
M-5	AMPR	24.6737576	23523.73	4.37150624
M-6	AMPR	27.7146854	2352.37	3.37150624
M-6	AMPR	27.983305	2352.37	3.37150624

* Amplification efficiency is 100.28%, $log_{10}(copies) = -0.3011*C_t + 11.828$, $R^2=0.9983$

Table S2 Statistical analysis using t.test functions for photo-sterilization of ARB

p-value	N-hem & C-hem	N-goe & C-goe
15 MIN	0.1715	0.03805
30 MIN	0.009011	0.053

* The p-value is calculated based on the comparison of bactericidal rate between natural and synthetic catalysts.

Table S3 Statistical analysis using TukeyHSD functions for photo-sterilization of ARB

p-value	N-hem	C-hem	N-goe	C-goe
15 MIN-0 MIN	3.63E-06	0.05955	0.001797	0.003346
30 MIN-0 MIN	0.0006757	0.003135	0.004428	0.01796
30 MIN-15 MIN	0.09946	0.9257	0.4019	0.9702

* The p-value is calculated based on the calculation of the bactericidal rate by a single catalyst at 0 min, 15 min, 30 min.

Table S4 Statistical analysis using TukeyHSD functions photodegradation effects on eARGs

p-value	N-hem	C-hem	N-goe	C-goe
15 MIN-0 MIN	0.0026982	0.0630685	0.0001467	0.0040763
30 MIN-0 MIN	0.0004449	0.0263038	0.0000102	0.001172
30 MIN-15 MIN	0.3815482	0.8433087	0.0491178	0.533442

* The p-value is calculated based on the calculation of the degradation amount of eARGs by a single catalyst at 0 min, 15 min, 30 min.

Table S5 Statistical analysis using t.test functions photodegradation effects on eARGs

p-value	N-hem & C-hem	N-goe & C-goe
15 MIN	1.02E-10	6.72E-06
30 MIN	3.36E-07	2.771E-11

* The p-value is calculated based on the calculation of the degradation amount of eARGs by NNIOs and synthetic ones).

Table S6 The conductive doped elements in NNIOs (mg/kg)

Sample Name	Mn	Ti	Co	Ni
N-hem	3463.405	4572.751	82.33895362	1088.091412
N-goe	233.0165	3207.155	9.543344	294.1108

Reference:

1. Li, D.; Hu, X.; Sun, Y.; Su, S.; Xia, A.; Ge, H., Goethite (α-FeOOH) nanopowders synthesized via a surfactant-assisted hydrothermal method: morphology, magnetic properties and conversion to rice-like α-Fe2O3 after annealing. **2015,** *5* (34), 2791-2796.

2. Tang, Z.; Wu, L.; Luo, Y.; Christie, P., Size fractionation and characterization of nanocolloidal particles in soils. *Environmental Geochemistry and Health* **2009,** *31* (1), 1-10.

3. Zhang, Z.; Tsuchimochi, T.; Ina, T.; Kumabe, Y.; Muto, S.; Ohara, K.; Yamada, H.; Ten-No, S. L.; Tachikawa, T., Binary dopant segregation enables hematite-based heterostructures for highly efficient solar H2O2 synthesis. *Nature Communications* **2022,** *13* (1), 1499.

4. Norrish, K.; Taylor, R. M., THE ISOMORPHOUS REPLACEMENT OF IRON BY ALUMINIUM IN SOIL GOETHITES. *Journal of Soil Science* **1961,** *12* (2), 294-306.

5. Kämpf, N.; Schwertmann, U., The 5-M-NaOH Concentration Treatment for Iron Oxides in Soils. *Clays and Clay Minerals* **1982,** *30* (6), 401-408.

6. Singh, B.; Gilkes, R. J., Concentration of iron oxides from soil clays by 5 M NaOH treatment : the complete removal of sodalite and kaolin. *Clay minerals* **1991,** *26* (4), 463-472.

7. Shuman, L., Separating Soil Iron and Manganese-Oxide Fractions for Microelement Analysis1. *Soil Science Society of America Journal - SSSAJ* **1982,** *46*.

8. Chen, L.; Qian, Z.; Wen, S.; Huang, S., High-Gradient Magnetic Separation of Ultrafine Particles with Rod Matrix. *Mineral processing and extractive metallurgy review* **2013,** *34* (5), 340-347.

9. Li, R.; Chen, T.; Lu, J.; Hu, H.; Zheng, H.; Zhu, P.; Pan, X., Metal–organic frameworks doped with metal ions for efficient sterilization: Enhanced photocatalytic activity and photothermal effect. *Water research (Oxford)* **2023,** *229*, 119366.